

## Radical and Heck Cyclizations of Diastereomeric *o*-Haloanilide Atropisomers

David B. Guthrie, Steven J. Geib, and Dennis P. Curran\*

Department of Chemistry, University of Pittsburgh, Pittsburgh, Pennsylvania 15261, United States

Received September 29, 2010; E-mail: curran@pitt.edu

**Abstract:** The outcomes of radical cyclizations and Heck reactions of *N*-(cyclohex-2-enyl)-*N*-(2-iodophenyl)acetamides depend critically on the configurations of the chiral axis and the stereocenter. In substrates without an *ortho*-methyl group, the diastereomeric precursors interconvert slowly at ambient temperatures. Cyclization of enriched mixtures of diastereomers provided similar yields of acetyl tetrahydrocarbazoles or dihydrocarbazoles, suggesting that interconversion of the radical or organometallic intermediates also occurs. Diastereomers of *N*-(cyclohex-2-enyl)-*N*-(2-iodo-4,6-dimethylphenyl)acetamides with an additional *ortho*-methyl group did not interconvert at ambient temperatures and were readily resolved. In radical cyclizations, *syn* diastereomers were prone to cyclize, while *anti* isomers were not. Strikingly, Heck reactions gave the opposite result; *anti* isomers were prone to cyclization and *syn* isomers were not. Heck reactions of allylic acetates occur with  $\beta$ -hydride elimination when acetate is *trans* to palladium and with  $\beta$ -acetoxy elimination when acetate is *cis*. This is surprising because prior studies have suggested that a *trans* relationship of palladium and acetoxy is essential for acetate elimination. Analyses of the results provide insights into mechanisms for radical cyclization and for insertion and elimination in the Heck reaction.

### Introduction

Radical cyclizations of axially chiral *o*-haloanilides typically occur with high chirality transfer from the axis to the new stereocenter. In one major class of reactions, cyclizations of acryloyl anilides provide 2-indolones with a new stereocenter in high selectivity.<sup>1</sup> This chirality transfer is not perturbed by nearby stereocenters. For example, valine-derived (*M,S*)-**1** and (*P,S*)-**1** can be separated and cyclized to give predominantly (*R,S*)-**2** and (*S,S*)-**2**, respectively (Figure 1).<sup>2</sup> The chiral axis, not the nearby stereocenter, controls the outcome, so either configuration of the new stereocenter in **2** can be accessed from a single enantiomer of valine.

Likewise, radical cyclizations of *N*-allyl-*o*-haloanilides also occur with high chirality transfer (Figure 2).<sup>3</sup> For example, cyclization of (*M*)-**3** provides (*R*)-**4** with high chirality transfer. This result shows that no rotation about the N–Ar bond occurs in the radical intermediate and that there is a facially selective cyclization. The transition-state model for such cyclizations is shown in **5**. Related anionic cyclizations and Heck reactions are similarly stereoselective.<sup>4,5</sup>

We were interested in perturbing such cyclizations by replacing one of the hydrogen atoms on the N–CH<sub>2</sub> group with

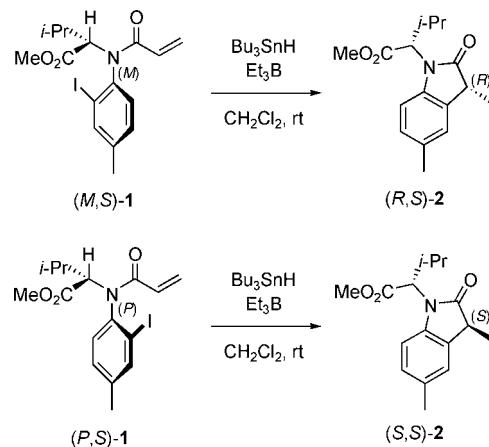


**Figure 1.** Radical cyclizations of diastereomeric valine-derived *o*-iodoanilides.

a substituent, resulting in diastereomers as shown in **6a,b**. Unlike **1** in Figure 1, whose stereocenter is extraannular (outside of the forming ring), the new stereocenters of **6a,b** are intraannular (part of the forming ring). Is the outcome of these cyclizations controlled by the chiral axis, the stereocenter, or both? There are two examples of such reactions in the literature;<sup>6,7</sup> however, it is not currently clear what controls selectivity.

Here we describe the results of a detailed study of radical cyclizations of *N*-cyclohexenyl-*o*-iodoanilides. It turns out that

- (1) (a) Curran, D. P.; Liu, W. D.; Chen, C. H.-T. *J. Am. Chem. Soc.* **1999**, *121*, 11012–11013. (b) Ates, A.; Curran, D. P. *J. Am. Chem. Soc.* **2001**, *123*, 5130–5131. (c) Petit, M.; Geib, S. J.; Curran, D. P. *Tetrahedron* **2004**, *60*, 7543–7552.
- (2) (a) Jones, K.; McCarthy, C. *Tetrahedron Lett.* **1989**, *30*, 2657–2660. (b) Petit, M.; Lapierre, A. J. B.; Curran, D. P. *J. Am. Chem. Soc.* **2005**, *127*, 14994–14995.
- (3) Curran, D. P.; Chen, C. H. T.; Geib, S. J.; Lapierre, A. J. B. *Tetrahedron* **2004**, *60*, 4413–4424.
- (4) Guthrie, D. B.; Curran, D. P. *Org. Lett.* **2009**, *11*, 249–251.
- (5) Lapierre, A. J. B.; Geib, S. J.; Curran, D. P. *J. Am. Chem. Soc.* **2007**, *129*, 494–495.

- (6) (a) Alcaide, B.; Almendros, P.; Rodríguez-Vicente, A.; Ruiz, M. P. *Tetrahedron* **2005**, *61*, 2767–2778. (b) Alcaide, B.; Moreno, A. M.; Rodríguez-Vicente, A.; Sierra, M. A. *Tetrahedron: Asymmetry* **1996**, *7*, 2203–2206.
- (7) Lampard, C.; Murphy, J. A.; Rasheed, F. *Tetrahedron Lett.* **1994**, *35*, 8675–8678.

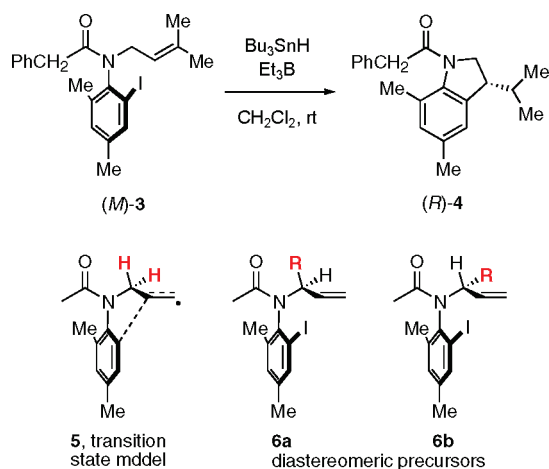


**Figure 2.** Example of chirality transfer in radical cyclizations of *N*-allyl-*o*-haloanilides, transition-state model **5** showing diastereotopic hydrogens targeted for replacement, and diastereomeric precursors **6a,b** of cyclizations with potential for intraannular chirality transfer.

both the chiral axis and the stereocenter are important in controlling the outcome of the reaction. This results in cyclizations of diastereomeric precursors that give structurally different products (rather than diastereomeric products) with very high selectivity.<sup>8</sup> We have previously reported one example of such a reaction in the context of a new radical phosphorylation with memory of chirality.<sup>9</sup> Here we report rotation barriers, crystal structures, and tin hydride experiments that allow us to understand this result.

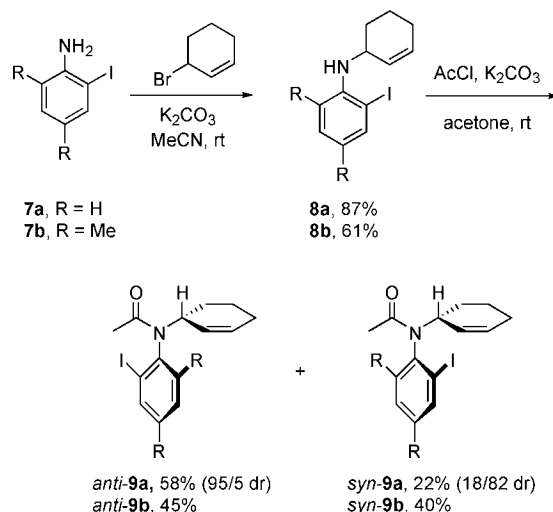
We also extend the study to Heck cyclizations<sup>10</sup> of the same precursors with surprising results. Again, diastereomeric precursors react to give different (rather than stereoisomeric) products, but the pathways of the Heck reactions are not anticipated by the radical cyclizations. The results provide insights into both the insertion and  $\beta$ -hydride elimination steps of the Heck reaction.<sup>11</sup>

## Results and Discussion

**Synthesis and Configuration of Atropisomeric *N*-Cyclohexenyl-*o*-iodoanilides.** Introduction of a stereocenter on the allyl substituent of an axially chiral anilide provides products with two stereocenters and therefore introduces a new element of diastereoselectivity in subsequent cyclizations. To simplify this aspect, we chose an *N*-cyclohexenyl substituent, which was expected to provide only products with a *cis* ring fusion.<sup>12</sup> Two pairs of diastereomeric anilides—with and without *ortho*-methyl substituents—were prepared as shown in Scheme 1.

2-Iodoaniline **7a** was alkylated with racemic 3-bromocyclohexene to produce *N*-cyclohexenyl aniline **8a** in 87% yield. This

**Scheme 1.** Synthesis of Diastereomeric *o*-Iodoanilides



was then acylated with acetyl chloride to produce a mixture of atropisomers **9a**. The two diastereomers were partially separable by column chromatography; the first eluting compound, *anti*-**9a**, was isolated in 58% yield in a 95/5 dr (*anti*-to-*syn* ratio). The second eluting compound, *syn*-**9a**, was collected in 22% yield in an 18/82 dr. The inability to isolate atropisomerically pure samples of **9a** is due to competitive *N*-Ar bond rotation during chromatography and isolation (see below).

The pair of *o,p*-dimethylated substrates **9b** was made in the same fashion. Alkylation of **7b** with 3-bromocyclohexene afforded **8b** in 61% yield. Acylation with acetyl chloride produced two diastereomers of **9b**, which were separated by flash chromatography. Less polar *anti*-**9b** (45% yield) was followed by *syn*-**9b** (40% yield). There is no interconversion of these atropisomers during isolation, so the samples are isomerically pure.

Single crystals of both *syn*- and *anti*-**9b** were grown by slow evaporation from a 3:1 hexane:CH<sub>2</sub>Cl<sub>2</sub> solvent mixture, and the X-ray crystal structures were solved. Isomer *anti*-**9b** crystallized with a pair of enantiomers in the unit cell; the (*P,R*) structure is shown in Figure 3. In this structure, the planes of the amide group and the aromatic ring are nearly perpendicular, with a dihedral angle of 84.1°. The *N*-cyclohexenyl bond is rotated such that the hydrogen  $\alpha$  to the amide nitrogen is pointing toward the *o*-iodine. The dihedral angle between this C–H bond and the *N*-carbonyl amide bond is 46.6°. The cyclohexene ring exists in a half-chair conformation with the amide group in a pseudoaxial position. In this structure, the iodine atom is held away from the alkene, implying that the radical derived from *anti*-**9b** is not predisposed for cyclization.

Slow evaporation of a solution containing racemic *syn*-**9b** deposited several crystals. The one chosen for analysis consisted

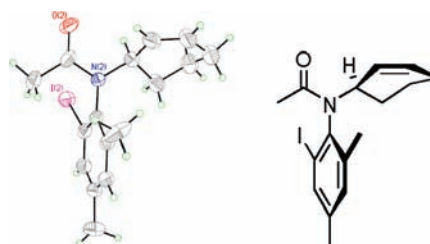


**Figure 3.** ORTEP and traditional representations of *anti*-**9b**.

- (8) Kumar, R. R.; Kagan, H. B. *Adv. Synth. Catal.* **2010**, *352*, 231–242.  
 (9) Bruch, A.; Ambrosius, A.; Fröhlich, R.; Studer, A.; Guthrie, D. B.; Zhang, H.; Curran, D. P. *J. Am. Chem. Soc.* **2010**, *132*, 11452–11454.  
 (10) (a) *The Mizoroki-Heck Reaction*; Oestreich, M., Ed.; John Wiley & Sons: Chichester, U.K., 2009. Gooffen, L.; Baumann, K. In *Handbook of C-H Transformations*; Dyker, G., Ed.; Wiley-VCH: Weinheim, 2005; pp 277–286. (b) Alonso, D. A.; Nájera, C. In *Compounds with All-Carbon Functions. Alkenes*; de Meijere, A., Ed.; Georg Thieme Verlag: Stuttgart, 2009; Vol. 47a, pp 439–479.  
 (11) (a) Jutand, A. In *The Mizoroki-Heck Reaction*; Oestreich, M., Ed.; John Wiley & Sons: Chichester, U.K., 2009; pp 1–50. (b) Knowles, J. P.; Whiting, A. *Org. Biomol. Chem.* **2007**, *5*, 31–44.  
 (12) Curran, D. P.; Porter, N. A.; Giese, B. *Stereochemistry of Radical Reactions: Concepts, Guidelines, and Synthetic Applications*; VCH: Weinheim, 1996; pp 51–71.

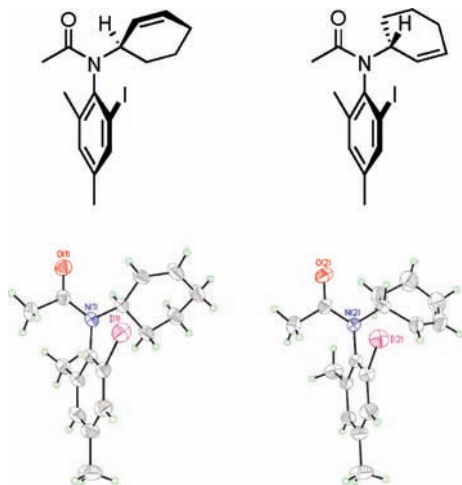


**Figure 4.** ORTEP and traditional representations of the two crystal forms of *syn-9b*.

of only the (*M,R*) enantiomer, containing two unique structures in the unit cell (Figure 4). In both structures the *N*-aryl plane was again nearly perpendicular to the plane of the amide, with dihedral angles of 84.8° and 85.6°. However, the two structures differ in the orientation of the *N*-cyclohexenyl group. In the left structure of Figure 4, the allylic hydrogen  $\alpha$  to nitrogen is pointed toward the *ortho*-methyl group, with a dihedral angle C–H $_{\alpha}$ –N–carbonyl of 48.5°. In the right structure, the  $\alpha$ -hydrogen is oriented toward the *o*-iodine, and the dihedral angle between the C–H $_{\alpha}$  bond and carbonyl–N bond is –41.5°. This molecule showed only one set of resonances in <sup>1</sup>H NMR spectra, so it is likely that these conformations rapidly interconvert in solution. Importantly, the *o*-iodine radical precursor is near the alkene, so the radical derived from *syn-9b* seems predisposed to cyclize.

The chromatographic and spectroscopic behavior of *syn*- and *anti-9b* allowed us to characterize atropisomeric compounds **9a** as *anti* or *syn* by analogy. During column chromatography on silica gel, *anti-9b* was less polar than *syn-9b*. Furthermore, <sup>1</sup>H NMR spectroscopy showed that the alkenyl and allylic ( $\alpha$  to N) protons of *anti-9b* were shifted downfield relative to those of *syn-9b*. After separation of the atropisomers of **9a**, the first eluting atropisomer indeed showed a downfield shift for the three diagnostic signals, so it is *anti-9a*. This pattern held true for all *N*-cyclohexenyl-*o*-iodoanilides prepared.

**Rotation Barriers of the *N*-Aryl Bonds of **9**.** Because *anti-9a* and *syn-9a* are diastereomers, their interconversion by rotation of the *N*-aryl bond occurs with two different barriers to rotation if  $K_{eq} \neq 1$ . To determine the barriers, a sample of *syn-9a* (28/72 dr) in a 9:1 hexanes/EtOAc solution was heated at 36 °C, and aliquots were periodically analyzed by HPLC. The final composition of the equilibrium mixture of **9a** was 65/35 *anti*/*syn*. The first-order isomerization of *syn-9a* to *anti-9a* was plotted against time (Figure 5).

The slope of the graph in Figure 5 corresponds to the rate constant of rotation from *syn-9a* to *anti-9a* (Figure 6) at 36 °C;  $k_1 = 5.2 \times 10^{-4} \text{ s}^{-1}$ . From the equilibrium values, the rate constant for the reverse rotation is  $k_{-1} = 2.8 \times 10^{-4} \text{ s}^{-1}$ . The barriers to rotation for these two processes at 36 °C are  $\Delta G^{\ddagger}_{rot} = 22.8$  and 23.1 kcal/mol, respectively. These values are

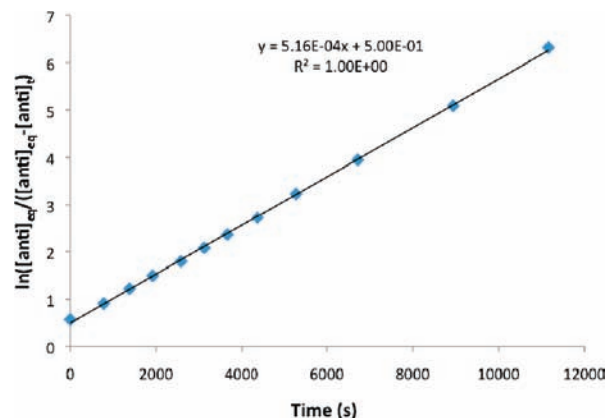


**Figure 5.** Equilibration plot of *syn-9a* and *anti-9a* over time.

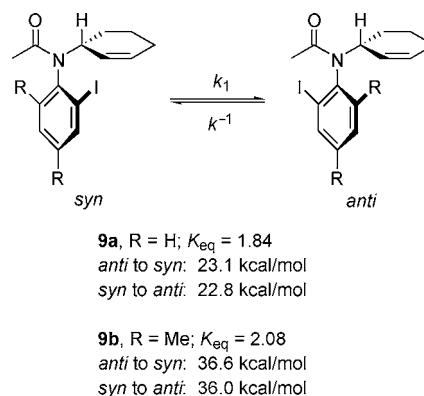


**Figure 6.** Barriers to rotation for *N*-cyclohexenyl atropisomers of **9a,b**.

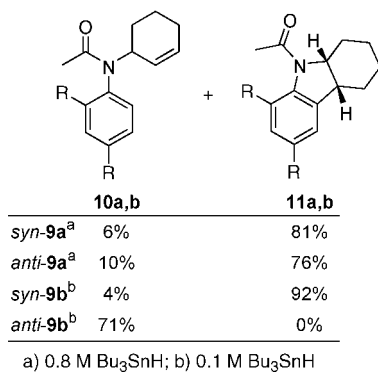
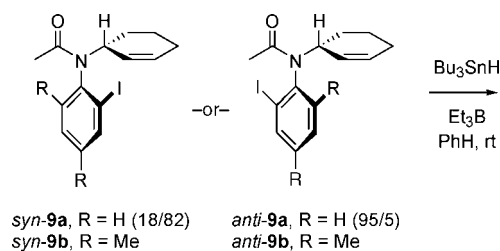
comparable to the experimentally determined barrier to rotation for a related *N*-cyclohexyl *o*-iodoanilide.<sup>13</sup>

The barriers to rotation for **9b** were determined in the same manner. However, **9b** is much more stable, and heating to 153 °C was necessary to effect rotation on a practical time scale (see Supporting Information). The rotation of *syn-9b* to *anti-9b* has a barrier of  $\Delta G^{\ddagger}_{rot} = 36.0$  kcal/mol, and the reverse process has  $\Delta G^{\ddagger}_{rot} = 36.6$  kcal/mol.

**Radical Reactions of *N*-Cyclohexenyl Atropisomers **9a,b**.** We next subjected both atropisomers of **9a** and **9b** to typical tin hydride reductions (Scheme 2). An 18/82 *anti*/*syn* mixture of **9a** was dissolved in a minimal amount of benzene with Bu<sub>3</sub>SnH, and Et<sub>3</sub>B initiator was added rapidly to the stirred solution (Scheme 2). Despite the high initial concentration of tin hydride ([Bu<sub>3</sub>SnH]<sub>0</sub> = 0.8 M), the cyclization product **11a** was isolated in 81% yield. The direct reduction product **10a** was isolated in only 6% yield. When the 95/5 *anti*/*syn* mixture of **9a** was reacted under the same conditions, similar results were obtained. Cyclized **11a** was isolated in 76% yield, and directly reduced **10a** was collected in 10% yield.

The Bu<sub>3</sub>SnH-mediated radical reactions of the pure atropisomers of **9b** gave strikingly different results. Reduction of *syn-9b* with Bu<sub>3</sub>SnH (0.10 M) and Et<sub>3</sub>B gave cyclized **11b** in 92% yield along with only 4% of reduced **10b**. This was an inseparable mixture of atropisomers in a 2:1 ratio, although the configurations of the atropisomers were not assigned. To confirm the identity of **10b**, catalytic hydrogenation over Pd/C produced

(13) Adler, T.; Bonjoch, J.; Clayden, J.; Font-Bardía, M.; Pickworth, M.; Solans, X.; Solé, D.; Vallverdú, L. *Org. Biomol. Chem.* **2005**, *3*, 3173–3183.

Scheme 2. Tin Hydride Reductions of *syn*- and *anti*-**9a,b**

an *N*-cyclohexylanilide with a simpler spectrum (see Supporting Information). In contrast, tin hydride reduction of *anti*-**9b** gave **10b** in 71% yield, again as a 2:1 mixture of atropisomers. Decreasing the Bu<sub>3</sub>SnH concentration 100-fold gave a crude product that was not as clean. Analysis of the <sup>1</sup>H NMR spectrum of this product showed significant amounts of **10b**, but no cyclized **11b**. A reaction in refluxing benzene, initiated by AIBN, gave similar results to this room-temperature experiment. In short, we could not detect formation of **11b** from *anti*-**9b** at any concentration or temperature studied.

Figure 7 shows an analysis of the results of cyclizations of **9a,b**. *ortho*-Methyl substrates *syn/anti*-**9b** give different products, so their derived radicals *syn/anti*-**12b** do not interconvert by N–Ar bond rotation. When radical *syn*-**12b** is formed (Figure 7), the preferred conformation of the cyclohexenyl group holds the alkene close to the radical in a geometry similar to that of

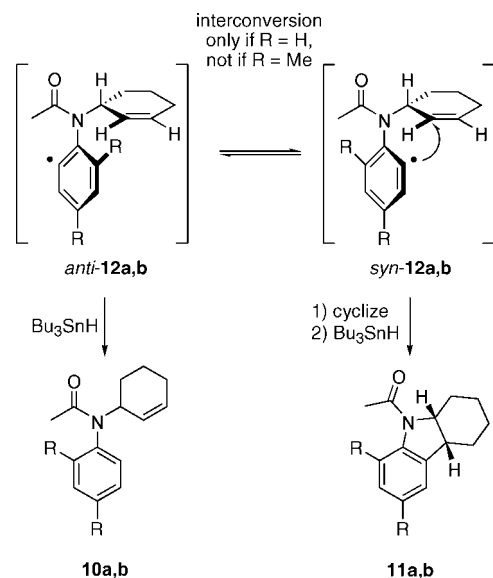


Figure 7. Competitive reactions of atropisomeric radicals **12a,b**.

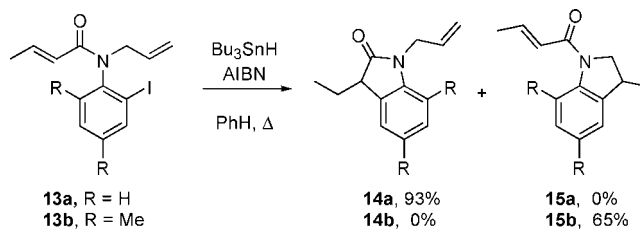


Figure 8. Regioselectivity in cyclizations of **13a,b** depends on the *o*-substituent.

TS model **5** (Figure 2). Rapid cyclization and subsequent reaction with tin hydride gives **11b**. The failure of *anti*-**12b** to cyclize in competition with reduction (even at low tin hydride concentration) is surprising. Its N–Ar bond cannot rotate, so it cannot access the transition state of *syn*-**12b**. Transition states for cyclization are apparently inaccessible by rotation of the *N*-cyclohexenyl bond. These transition states do not resemble **5** in geometry and must be rather high in energy.

By analogy to the results with **12b** (R = Me), radical *syn*-**12a**, which lacks the *ortho*-methyl group (R = H), is prone to cyclize, while *anti*-**12a** is not. Because *anti*-**9a** and *syn*-**9a** give similar results at high tin hydride concentration, the interconversion of *anti/syn*-**12a** must be rapid relative to the onward reaction. Assuming that *anti*-**12a** does not cyclize directly, at least 75% of *anti*-**12a** must have undergone rotation to *syn*-**12a** to account for the total yield of **11a**. This implies that the rotation process interconverting *anti*-**12a** and *syn*-**12a** is at least three times faster than the competing reduction by Bu<sub>3</sub>SnH.

The rate constant  $k_H$  for reduction of the phenyl radical is  $5.2 \times 10^8 \text{ M}^{-1} \text{ s}^{-1}$  at room temperature.<sup>14</sup> In the experiments shown in Scheme 2, the mean tributyltin hydride concentration<sup>15</sup> [Bu<sub>3</sub>SnH]<sub>c</sub> = 0.55 M, so the rate of reduction of *anti*-**12a** is about  $2.9 \times 10^8 \text{ s}^{-1}$ . We can therefore identify a lower limit for the rotational rate constant of *anti*-**12a** to *syn*-**12a** of  $k_r = 8.7 \times 10^8 \text{ s}^{-1}$ .

**Radical Reactions of Diastereomeric Atropisomers with Two Acceptors.** Independent observations by Storey and Jones<sup>16</sup> and our group<sup>5,17</sup> have illuminated an unusual regioselectivity effect in the cyclizations of compounds with two radical acceptors such as **13a** and **13b** (Figure 8). When no second *ortho* substituent is present, as in **13a** (R = H), cyclization occurs exclusively onto the acryloyl group to give **14a** with no trace of **15a**. When an *ortho*-methyl group is present, however, **13b** (R = Me) cyclizes preferentially onto the *N*-allyl group to give **15b** with no **15a**. This difference was attributed to steric hindrance between the second *o*-substituent and the *N*-allyl group, which slows the cyclization onto the crotonyl group by disfavoring twisting of the N–Ar bond.<sup>5</sup>

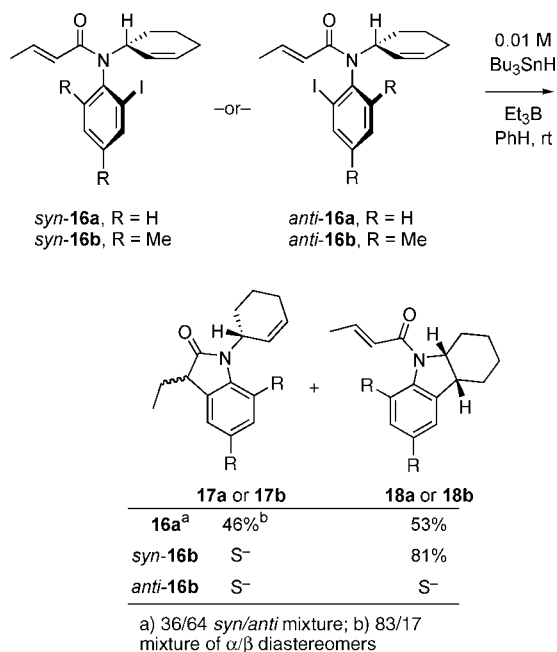
To address the question of how a stereocenter next to nitrogen influences this interesting regiodivergent behavior, we prepared substrates **16a** and **16b** with an additional alkene acceptor at the amide carbonyl (Scheme 3). While both atropisomers of **16a** (made from **8a**) were visible by TLC analysis, N–aryl bond rotation was too rapid for separation by flash chromatography, and **16a** was isolated as a 64/36 *anti/syn* mixture. Atropisomers

(14) Johnston, L. J.; Luszyk, J.; Wayner, D. D. M.; Abeywickreyma, A. N.; Beckwith, A. L. J.; Scaiano, J. C.; Ingold, C. K. *J. Am. Chem. Soc.* **1985**, *107*, 4594–4596.

(15) Newcomb, M. *Tetrahedron* **1993**, *49*, 1151–1176.

(16) Jones, K.; Storey, J. M. D. *J. Chem. Soc., Chem. Commun.* **1992**, 1766–1767.

(17) Lapiere, A. J. B. Ph.D. Dissertation, University of Pittsburgh, 2005.

**Scheme 3.** Radical Reactions of Substrates **16a,b** with Two Acceptors

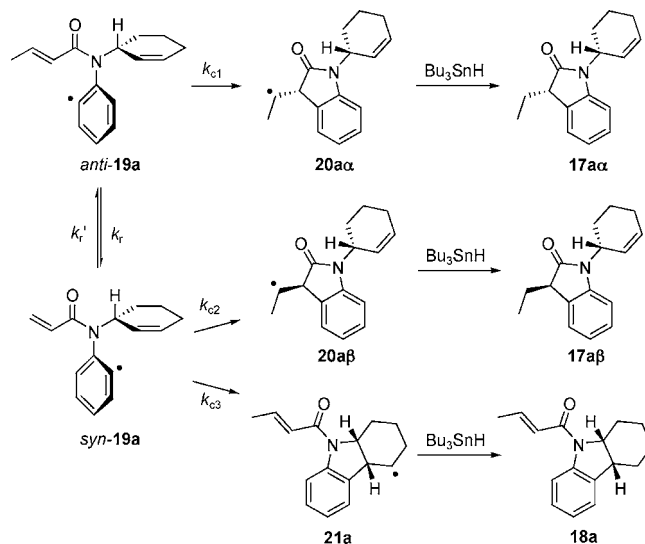
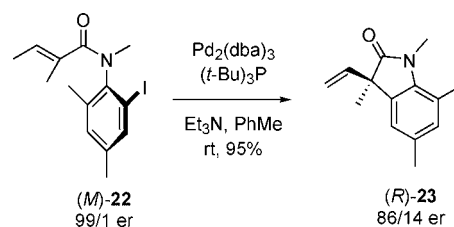
of *ortho*-methyl anilide **16b** were separable by column chromatography; *anti*-**16b** was isolated in 38% yield, and *syn*-**16b** was isolated in 29% yield.

These substrates were then reacted under radical conditions as shown in Scheme 3. When the 64/36 *anti/syn* mixture of **16a** was treated with Bu<sub>3</sub>SnH at room temperature, a mixture of products was formed. The first eluting *N*-cyclohexenylindolone, **17a**, was obtained in 46% yield as an inseparable 5:1 mixture of diastereomers. Tricycle **18a** was also collected in 53% yield.

Substrate *syn*-**16b** was reacted with Bu<sub>3</sub>SnH (0.01 M) and Et<sub>3</sub>B at room temperature in benzene to give **18b** in 81% yield as the sole product. There was no evidence for direct reduction (product not shown) or for formation of **17b**. The reaction of *anti*-**16b** under similar conditions gave a complex mixture of products in poor mass balance.

The results in the **16b** (R = Me) series are consistent with the observations of **13b** in Figure 8. Specifically, *syn*-**16b** has both the *ortho*-methyl group (favors cyclization to the *N*-allyl side) and the configuration at the stereocenter that is prone to cyclization. Because of these matched effects, a high yield of **18b** is obtained. But *anti*-**16b** has mismatched effects. The *ortho*-methyl group favors cyclization of the *N*-cyclohexenyl side, while the configuration of the stereocenter disfavors it. Indeed, neither cyclized product was observed in the crude reaction mixture.

Pathways for formation of **17a** and **18a** from **16a** are shown in Figure 9. Radical *anti*-**19a**, formed directly from *anti*-**16a**, should cyclize preferentially onto the crotonyl group to give cyclized radical **20a $\alpha$** , precursor of **17a $\alpha$** . This regioselectivity follows from the result with **13a** (Figure 8) and from the configuration (*anti*), which is mismatched for *N*-cyclohexenyl cyclization. The stereoselectivity follows from the usual model<sup>1,2</sup> (and has not been confirmed). Radical *syn*-**19a**, produced by iodine atom abstraction from *syn*-**16a**, has two cyclization pathways available. Cyclization onto the crotonyl group (as with **13a**) gives radical **20a $\beta$** , leading to product **17a $\beta$** . Alternatively, the *syn*-configuration is matched for cyclization onto the

**Figure 9.** Pathways for reactions of radicals derived from **16a**.**Figure 10.** Room-temperature Heck reaction of an axially chiral substrate.

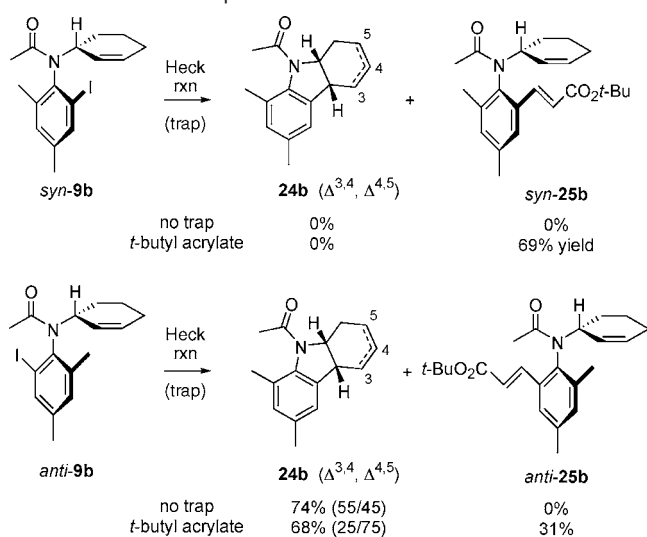
cyclohexenyl group to produce radical **21a**, which leads to **18a**. Aryl radicals *anti*-**19a** and *syn*-**19a** may also interconvert by an *N*-aryl bond rotation, as shown by the prior results (Figure 7).

If the *N*-aryl rotation processes of *anti*-**19a** and *syn*-**19a** ( $k_r$ ,  $k_r'$ ) are significantly slower than cyclization processes ( $k_{c1}$ ,  $k_{c2}$ ,  $k_{c3}$ ), then the ratio of products **17a $\alpha$** /(**17a $\beta$**  + **18a**) should reflect the starting *anti/syn* ratio of 64/36. However, this is not the case. For example, the yield of **18a** (53%) significantly exceeds the percentage of its precursor *syn*-**16a** (36%). Therefore, *anti*-**19a** and *syn*-**19a** must equilibrate to some extent at room temperature before cyclizing.

**Heck Reactions of Diastereomeric Atropisomers.** We have previously investigated chirality transfer in room-temperature Heck reactions of axially chiral *o*-iodoanilides (Figure 10).<sup>5</sup> In these reactions, the axis of chirality of the substrates dictated the stereochemistry of the product. For example, cyclization of (*M*)-**22** gives (*R*)-**23** with about 86% chirality transfer.

Because substrates **9b** have restricted rotation about both the *N*-aryl and *N*-cyclohexenyl bonds, we surmised on the basis of the radical results that one atropisomer would cyclize under Heck conditions, while the other would not. In the event, this prediction was realized, but in the reverse! We subjected both diastereomers of **9b** to the room-temperature Heck conditions of Hartwig (Scheme 4).<sup>18</sup> When *syn*-**9b** was treated with catalytic Pd<sub>2</sub>(dba)<sub>3</sub> and P(*t*-Bu)<sub>3</sub> ligand with Et<sub>3</sub>N base, no cyclization to **24b** occurred. Conducting a similar reaction of *syn*-**9b** in the presence of excess *tert*-butyl acrylate (to trap aryl-Pd intermediates) provided bimolecular Heck adduct *syn*-**25b**

(18) Stambuli, J. P.; Stauffer, S. R.; Shaughnessy, K. H.; Hartwig, J. F. *J. Am. Chem. Soc.* **2001**, *123*, 2677–2678.

Scheme 4. Room-Temperature Heck Reactions of **9b**<sup>a</sup>

<sup>a</sup> Conditions: 10 mol % Pd<sub>2</sub>(dba)<sub>3</sub>·CHCl<sub>3</sub>, 40 mol % P(*t*-Bu)<sub>3</sub>·HBF<sub>4</sub>, Et<sub>3</sub>N, DMF, rt, with or without trap.

in 69% yield. Notice that the axial chirality is retained in this bimolecular process.<sup>9</sup> The room-temperature Heck reaction of *anti*-**9b** effected intramolecular cyclization, producing 74% of **24b** as an inseparable mixture of alkene isomers in a 55:45 ratio. Performing the Heck reaction of *anti*-**9b** in the presence of *tert*-butyl acrylate formed trapped adduct *anti*-**25b** in 31% yield along with **24b** in 68% yield (25/75 mixture of alkene isomers). Again, the bimolecular product **25b** was found with retention of axial chirality.

In contrast to the radical reactions of **9b**, in which only the *syn* atropisomer is prone to cyclize, only *anti*-**9b** is prone to cyclize under room-temperature Heck conditions. We suggest that this dramatic difference originates from fundamental differences in the radical and Heck reaction transition-state geometries. In the radical reaction, only two atoms need to approach: the radical center and the alkene carbon being attacked. The usual trajectory for approach ( $\sim 109^\circ$  attack angle)<sup>19</sup> is readily accommodated from the *syn* radical.

However, in the insertion step of the Heck reaction, four atoms come together: both atoms of the C<sub>Ar</sub>–Pd bond approach both atoms of the alkene.<sup>11</sup> This approach is not easily accommodated from the *syn* precursor because the Pd atom is placed under the ring rather than near the alkene.<sup>20</sup>

A proposed pathway for the Heck cyclization of *anti*-**9b** is shown in Figure 11. Oxidative addition of the palladium catalyst into the carbon–iodine bond of *anti*-**9b** produces arylpalladium intermediate **26**. N–aryl rotation, concomitant with N–cyclohexenyl bond rotation, allows for coordination between the palladium and the alkene on the concave face of the cyclohexene ring, as in **27**. All four key participating atoms are well positioned, and migratory insertion from this face results in *cis*-fused intermediate **28**. Only one hydrogen is available for *syn*  $\beta$ -hydride elimination, so **24b**  $\Delta^{3,4}$  is presumably the primary product. Subsequent palladium hydride reinsertion and elimination can migrate the double bond to the  $\Delta^{4,5}$  position.

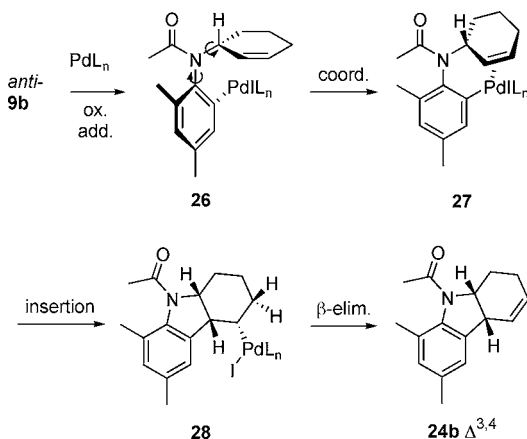


Figure 11. Proposed pathway for Heck cyclization of *anti*-**9b**.

**Radical and Heck Reactions of N-Cyclohexenyl Allylic Acetates.** In the final step of the Heck reaction, the  $\beta$ -elimination of a heteroatomic leaving group (for example, –Cl, –OAc, –OCH<sub>3</sub>) typically proceeds more quickly than competing  $\beta$ -hydride elimination when both pathways are available.<sup>21</sup> Recently, Lautens and co-workers developed a procedure for the efficient Heck coupling of aryl iodides and allylic acetates.<sup>22</sup> The final step of this reaction presumably involves a chemoselective  $\beta$ -acetoxy elimination. Very little isomerization of the double bond was seen in most products. We wondered whether judicious placement of an acetoxy group in such substrates could avoid a palladium hydride intermediate, thereby circumventing isomerization.

With this in mind, a series of disubstituted cyclohexenes containing a *cis*- or a *trans*-acetoxy group relative to the anilide group were prepared as described in the Supporting Information. The precursor structures and the products from radical and Heck cyclizations are summarized in Table 1. In the *ortho*-methyl series (**27c,t**), separation was possible and the atropisomers were stable. The *syn* and *anti* isomers of **26c** and **26t** (*ortho*-hydrogen substituent) could not be separated. However, upon standing at room temperature, a sample of neat oil **26c** (60/40, *anti*/*syn*) spontaneously formed crystals possessing the *anti* configuration (Figure 12). The selective crystallization of one diastereomeric atropisomer, a dynamic thermodynamic resolution, has been performed previously to produce diastereoenriched anilides from an equilibrium mixture.<sup>1b</sup> The torsion angle between the amide and aromatic planes of *anti*-**26c** is 83.8°, essentially perpendicular, as expected. The cyclohexene ring exists in a half-chair conformation with the bulkier amide group pseudoequatorial and the acetate pseudoaxial. <sup>1</sup>H NMR analysis by dissolution of a crystal at low temperature (see Supporting Information) confirmed that *anti*-**26c** is the major atropisomer in CDCl<sub>3</sub> solution after equilibrium is reached.

Under tin hydride conditions (Table 1), all compounds containing an allylic acetate group behaved similarly to unsubstituted analogue **9a** or **9b**. *trans*-Disubstituted **26t** (60/40 *anti*/*syn*) provided tricycle **28t** in 89% yield. Similarly, *cis* isomer

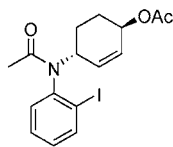
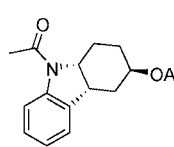
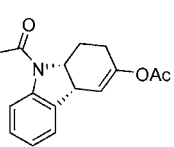
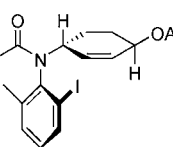
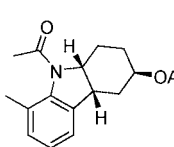
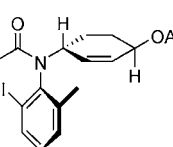
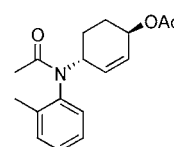
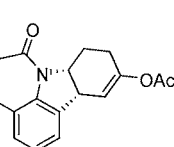
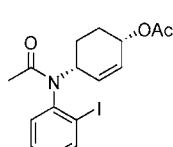
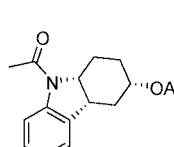
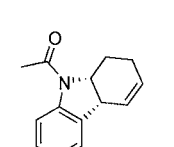
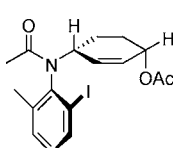
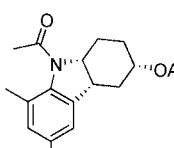
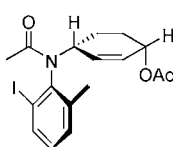
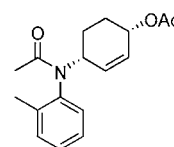
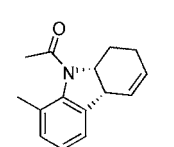
(19) Beckwith, A. J. J.; Schiesser, C. H. *Tetrahedron* **1985**, *41*, 3925–3941.

(20) (a) Mori, M.; Nakanishi, M.; Kajishima, D.; Sato, Y. *Org. Lett.* **2001**, *3*, 1913–1916. (b) Mori, M.; Nakanishi, M.; Kajishima, D.; Sato, Y. *J. Am. Chem. Soc.* **2003**, *125*, 9801–9807.

(21) Zhu, G.; Lu, X. *Organometallics* **1995**, *14*, 4899–4904.

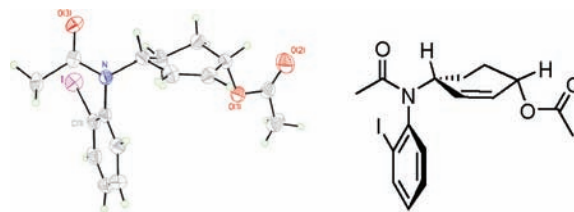
(22) (a) Mariampillai, B.; Herse, C.; Lautens, M. *Org. Lett.* **2005**, *7*, 4745–4747. (b) Lautens, M.; Tayama, E.; Herse, C. *J. Am. Chem. Soc.* **2005**, *127*, 72–73. (c) Similar selectivities in  $\beta$ -eliminations have been observed by Dr Christelle Herse of the University of Toronto as cited in the Thesis of Dr. Brian Mariampillai, University of Toronto, pp 158–159, 2009. We thank Prof. Mark Lautens for sharing this information.

**Table 1.** Radical and Heck Cyclizations of Allylic Acetates

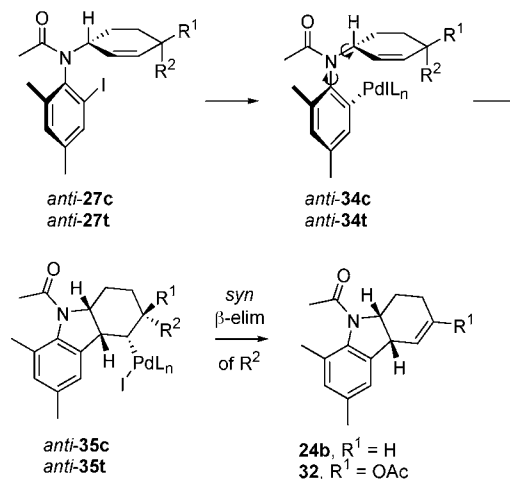
Precursor	Radical Product <sup>a</sup>	Heck Product <sup>b</sup>
 <b>26t</b> (60/40 <i>anti/syn</i> )	 <b>28t</b> , 89%	 <b>31</b> , 47%
 <i>syn</i> - <b>27t</b>	 <b>29t</b> , 77%	— <sup>d</sup>
 <i>anti</i> - <b>27t</b>	 <b>30t</b> , 96% <sup>c</sup> (67/33 atrop. ratio)	 <b>32</b> , 73%
 <b>26c</b> (60/40 <i>anti/syn</i> )	 <b>28c</b> , 92%	 <b>33</b> , 47%
 <i>syn</i> - <b>27c</b>	 <b>29c</b> , 71%	— <sup>d</sup>
 <i>anti</i> - <b>27c</b>	 <b>30c</b> , 96% <sup>c</sup> (67/33 atrop. ratio)	 <b>24b</b> , 47%

<sup>a</sup> 1.5 equiv of Bu<sub>3</sub>SnH, 1.0 equiv of Et<sub>3</sub>B, [Bu<sub>3</sub>SnH]<sub>i</sub> = 0.01 M, PhH, rt. <sup>b</sup> 5 mol % Pd<sub>2</sub>(dba)<sub>3</sub>, CHCl<sub>3</sub>, 22 mol % P(*o*-tol)<sub>3</sub>, BuNMe<sub>2</sub>, 10:1 MeCN/H<sub>2</sub>O sealed tube, 80 °C. <sup>c</sup> [Bu<sub>3</sub>SnH]<sub>i</sub> = 0.2 M. <sup>d</sup> Reaction not attempted.

**26c** (60/40 *anti/syn*) cyclized to **28c** in 92% yield. *ortho*-Methyl substrates *syn*-**27t** and *syn*-**27c** also underwent cyclization, producing **29t** (77% yield) and **29c** (71% yield), respectively. When *anti*-**27t** was treated with Bu<sub>3</sub>SnH at an initial hydride concentration of 0.01 M, multiple products were formed. However, increasing the [Bu<sub>3</sub>SnH]<sub>i</sub> to 0.20 M produced **30t** in 96% yield in a 67/33 ratio of atropisomers. Similarly, the radical

**Figure 12.** X-ray crystal structure of *anti*-**26c**.

**c**, *cis*-series, R<sup>1</sup> = H, R<sup>2</sup> = OAc  
**t**, *trans*-series, R<sup>1</sup> = OAc, R<sup>2</sup> = H

**Figure 13.** Suggested mechanism of Heck reaction with chemoselective  $\beta$ -elimination.

reaction of *anti*-**27c** afforded directly reduced **30c** (96% yield) as a 67/33 mixture of atropisomers. In short, the substrates lacking the *o*-Me group (**26c,t**) gave cyclized products in similar yields. When the *o*-Me group was present (**27c,t**), *syn*-isomers cyclized and *anti*-isomers did not.

Four of the substrates were then subjected to Heck conditions according to the procedure developed by Lautens.<sup>22</sup> In a typical experiment, **26t** (60/40 *anti/syn*) was combined in wet acetonitrile with BuNMe<sub>2</sub> and catalytic amounts of Pd<sub>2</sub>(dba)<sub>3</sub>·CHCl<sub>3</sub> and P(*o*-tol)<sub>3</sub>. The mixture was placed in a sealed tube and heated at 80 °C until Pd-black precipitated. After purification, tricyclic vinyl acetate **31** was isolated in 47% yield. Under the same reaction conditions, *anti*-**27t** produced **32** in 73% yield, again as the vinyl acetate. The behavior of *cis*-disubstituted cyclohexene systems under these conditions was studied as well. Under Heck conditions, **26c** (60/40 *anti/syn*) gave alkene **33** in 82% yield as the sole product. Similarly, *anti*-**27c** produced alkene **24b** in 73% yield. On the basis of the results with *syn*-**9b**, the *syn* atropisomers of **27t** and **27c** were expected to be unreactive toward Heck cyclizations, so these were not examined.

A mechanistic rationale for these results is shown in Figure 13 with substrates *anti*-**27c** and *anti*-**27t** as examples. Oxidative addition of the Pd<sup>0</sup> catalyst occurs to give aryl-Pd<sup>II</sup> intermediate **34c** or **34t**. Concomitant *N*-aryl and *N*-cyclohexenyl rotation followed by insertion gives alkylpalladium intermediate **35c** or **35t**. These undergo  $\beta$ -elimination with the *syn* substituent R<sup>2</sup>. In the reaction of *anti*-**27c**, R<sup>2</sup> in palladium intermediate **35c** is an acetate group, so IPd<sup>II</sup>OAc is eliminated to give alkene **24b**. When *anti*-**27t** is the substrate, R<sup>2</sup> in **35t** is H, and  $\beta$ -hydride elimination occurs to give vinyl acetate **32**.

The ability of **35t** to undergo  $\beta$ -acetoxy elimination when R<sup>2</sup> = OAc is unusual. Previous studies have shown that

$\beta$ -elimination of heteroatom substituents during the Heck reaction proceeds with the leaving group *anti*-periplanar to the palladium.<sup>18,19,23</sup> However, those studies were performed under acidic conditions, with Pd(OAc)<sub>2</sub> catalyst in AcOH solution. Both *anti*- and *syn*-eliminations of aryloxy groups have been observed during Heck reactions in the presence of trialkylamine base.<sup>22c,24</sup> The propensity for this system to undergo *syn*-acetoxy elimination is indicative of a change in preferred geometry for  $\beta$ -elimination under basic conditions.

### Conclusions

The results of radical cyclizations and Heck reactions of *N*-(3-cyclohexenyl)-*ortho*-iodoacetanilides depend critically on the configurations of the chiral axis and the stereocenter. In substrates **9a**, **13a**, **16a**, **26t**, and **26c** without an additional *ortho*-methyl group, the precursor diastereomers interconvert slowly at ambient temperatures. Radical and Heck cyclizations of enriched mixtures of diastereomers occurred in high yields and provided similar results, suggesting that interconversion of the radical or organometallic intermediates also occurs.

Diastereomers of substrates **9b**, **13b**, **16b**, **27t**, and **27c** with an additional methyl group did not interconvert at ambient

temperatures and were readily resolved. In radical cyclizations, the *syn*-diastereomers were prone to cyclize while the *anti* isomers were not (bimolecular reduction occurred instead). Strikingly, Heck reactions gave the opposite result; *anti* isomers were prone to cyclize and *syn* isomers preferred bimolecular reactions. Heck reactions of allylic acetates occur with  $\beta$ -hydride elimination when acetate is *trans* to palladium and with  $\beta$ -acetoxy elimination when acetate is *cis*. This is surprising because prior studies have suggested that a *trans* relationship of palladium and acetoxy was favored for acetate elimination.

These results show the dramatic effects that axial chirality can have on the outcome of radical cyclizations and Heck reactions. The effects can be either reinforced or negated by the additional stereocenter present in the substrates, thereby providing insight into geometries of intermediates and transition states.

**Acknowledgment.** We thank the U.S. National Science Foundations (NSF) for funding.

**Supporting Information Available:** Experimental procedures and compound characterization data. This material is available free of charge via the Internet at <http://pubs.acs.org>.

JA108795X

(23) Cheng, J. C.-Y.; Daves, J.; Doyle, G. *Organometallics* **1986**, *5*, 1753–1755.

(24) Sinou, D.; Bedjeglal, K. *Eur. J. Org. Chem.* **2000**, 4071–4077.